Observation of OZI-suppressed decays χcJ →ωφ

Observation of OZI-suppressed decays $\chi_{cJ} \to \omega\phi$

M. Ablikim,[1] M. N. Achasov,[10,d] S. Ahmed,[15] M. Albrecht,[4] M. Alekseev,[55a,55c] A. Amoroso,[55a,55c] F. F. An,[1] Q. An,[42,52] J. Z. Bai,[1] Y. Bai,[41] O. Bakina,[27] R. Baldini Ferroli,[23a] Y. Ban,[35] K. Begzsuren,[25] D. W. Bennett,[22] J. V. Bennett,[5] N. Berger,[26] M. Bertani,[23a] D. Bettoni,[24a] F. Bianchi,[55a,55c] E. Boger,[27,b] I. Boyko,[27] R. A. Briere,[5] H. Cai,[57] X. Cai,[1,42] O. Cakir,[45a] A. Calcaterra,[23a] G. F. Cao,[1,46] S. A. Cetin,[45b] J. Chai,[55c] J. F. Chang,[1,42] G. Chelkov,[27,b,c] G. Chen,[1] H. S. Chen,[1,46] J. C. Chen,[1] M. L. Chen,[1,42] P. L. Chen,[53] S. J. Chen,[33] X. R. Chen,[30] Y. B. Chen,[1,42] W. Cheng,[55c] X. K. Chu,[35] G. Cibinetto,[24a] F. Cossio,[55c] H. L. Dai,[1,42] J. P. Dai,[37,h] A. Dbeyssi,[15] D. Dedovich,[27] Z. Y. Deng,[1] A. Denig,[26] I. Denysenko,[27] M. Destefanis,[55a,55c] F. De Mori,[55a,55c] Y. Ding,[31] C. Dong,[34] J. Dong,[1,42] L. Y. Dong,[1,46] M. Y. Dong,[1] Z. L. Dou,[33] S. X. Du,[60] P. F. Duan,[1] J. Fang,[1,42] S. S. Fang,[1,46] Y. Fang,[1] R. Farinelli,[24a,24b] L. Fava,[55b,55c] S. Fegan,[26] F. Feldbauer,[4] G. Felici,[23a] C. Q. Feng,[42,52] E. Fioravanti,[24a] M. Fritsch,[4] C. D. Fu,[1] Q. Gao,[1] X. L. Gao,[42,52] Y. Gao,[44] Y. G. Gao,[6] Z. Gao,[42,52] B. Garillon,[26] I. Garzia,[24a] A. Gilman,[49] K. Goetzen,[11] L. Gong,[34] W. X. Gong,[1,42] W. Gradl,[26] M. Greco,[55a,55c] L. M. Gu,[33] M. H. Gu,[1,42] Y. T. Gu,[13] A. Q. Guo,[1] L. B. Guo,[32] R. P. Guo,[1,46] Y. P. Guo,[26] A. Guskov,[27] Z. Haddadi,[29] S. Han,[57] X. Q. Hao,[16] F. A. Harris,[47] K. L. He,[1,46] X. Q. He,[51] F. H. Heinsius,[4] T. Held,[4] Y. K. Heng,[1] Z. L. Hou,[1] H. M. Hu,[1,46] J. F. Hu,[37,h] T. Hu,[1] Y. Hu,[1] G. S. Huang,[42,52] J. S. Huang,[16] X. T. Huang,[36] X. Z. Huang,[33] Z. L. Huang,[31] T. Hussain,[54] W. Ikegami Andersson,[56] M. Irshad,[42,52] Q. Ji,[1] Q. P. Ji,[16,*] X. B. Ji,[1,46] X. L. Ji,[1,42] X. S. Jiang,[1] X. Y. Jiang,[34] J. B. Jiao,[36] Z. Jiao,[18] D. P. Jin,[1] S. Jin,[1,46] Y. Jin,[48] T. Johansson,[56] A. Julin,[49] N. Kalantar-Nayestanaki,[29] X. S. Kang,[34] M. Kavatsyuk,[29] B. C. Ke,[1] I. K. Keshk,[4] T. Khan,[42,52] A. Khoukaz,[50] P. Kiese,[26] R. Kiuchi,[1] R. Kliemt,[11] L. Koch,[28] O. B. Kolcu,[45b,f] B. Kopf,[4] M. Kornicer,[47] M. Kuemmel,[4] M. Kuessner,[4] A. Kupsc,[56] M. Kurth,[1] W. Kühn,[28] J. S. Lange,[28] P. Larin,[15] L. Lavezzi,[55c,1] S. Leiber,[4] H. Leithoff,[26] C. Li,[56] Cheng Li,[42,52] D. M. Li,[60] F. Li,[1,42] F. Y. Li,[35] G. Li,[1] H. B. Li,[1,46] H. J. Li,[1,46] J. C. Li,[1] J. W. Li,[40] K. J. Li,[43] Kang Li,[14] Ke Li,[1] Lei Li,[3] P. L. Li,[42,52] P. R. Li,[7,46] Q. Y. Li,[36] T. Li,[36] W. D. Li,[1,46] W. G. Li,[1] X. L. Li,[36] X. N. Li,[1,42] X. Q. Li,[34] Z. B. Li,[43] H. Liang,[42,52] Y. F. Liang,[39] Y. T. Liang,[28] G. R. Liao,[12] L. Z. Liao,[1,46] J. Libby,[21] C. X. Lin,[43] D. X. Lin,[15] B. Liu,[37,h] B. J. Liu,[1] C. X. Liu,[1] D. Liu,[42,52] D. Y. Liu,[37,h] F. H. Liu,[38] Fang Liu,[1] Feng Liu,[6] H. B. Liu,[13] H. L. Liu,[41] H. M. Liu,[1,46] Huanhuan Liu,[1] Huihui Liu,[17] J. B. Liu,[42,52] J. Y. Liu,[1,46] K. Liu,[44] K. Y. Liu,[31] Ke Liu,[6] L. D. Liu,[35] Q. Liu,[46] S. B. Liu,[42,52] X. Liu,[30] Y. B. Liu,[34] Z. A. Liu,[1] Zhiqing Liu,[26] Y. F. Long,[35] X. C. Lou,[1] H. J. Lu,[18] J. G. Lu,[1,42] Y. Lu,[1] Y. P. Lu,[1,42] C. L. Luo,[32] M. X. Luo,[59] T. Luo,[9,j] X. L. Luo,[1,42] S. Lusso,[55c] X. R. Lyu,[46] F. C. Ma,[31] H. L. Ma,[1] L. L. Ma,[36] M. M. Ma,[1,46] Q. M. Ma,[1] T. Ma,[1] X. N. Ma,[34] X. Y. Ma,[1,42] Y. M. Ma,[36] F. E. Maas,[15] M. Maggiora,[55a,55c] S. Maldaner,[26] Q. A. Malik,[54] A. Mangoni,[23b] Y. J. Mao,[35] Z. P. Mao,[1] S. Marcello,[55a,55c] Z. X. Meng,[48] J. G. Messchendorp,[29] G. Mezzadri,[24b] J. Min,[1,42] T. J. Min,[33] R. E. Mitchell,[22] X. H. Mo,[1] Y. J. Mo,[6] C. Morales Morales,[15] N. Yu. Muchnoi,[10,d] H. Muramatsu,[49] A. Mustafa,[4] S. Nakhoul,[11,g] Y. Nefedov,[27] F. Nerling,[11] I. B. Nikolaev,[10,d] Z. Ning,[1,42] S. Nisar,[8] S. L. Niu,[1,42] X. Y. Niu,[1,46] S. L. Olsen,[46] Q. Ouyang,[1] S. Pacetti,[23b] Y. Pan,[42,52] M. Papenbrock,[56] P. Patteri,[23a] M. Pelizaeus,[4] J. Pellegrino,[55a,55c] H. P. Peng,[42,52] Z. Y. Peng,[13] K. Peters,[11,g] J. Pettersson,[56] J. L. Ping,[32] R. G. Ping,[1,46] A. Pitka,[4] R. Poling,[49] V. Prasad,[42,52] H. R. Qi,[2] M. Qi,[33] T. Y. Qi,[2] S. Qian,[1,42] C. F. Qiao,[46] N. Qin,[57] X. S. Qin,[4] Z. H. Qin,[1,42] J. F. Qiu,[1] S. Q. Qu,[34] K. H. Rashid,[54,i] C. F. Redmer,[26] M. Richter,[4] M. Ripka,[26] A. Rivetti,[55c] M. Rolo,[55c] G. Rong,[1,46] Ch. Rosner,[15] A. Sarantsev,[27,e] M. Savrié,[24b] K. Schoenning,[56] W. Shan,[19] X. Y. Shan,[42,52] M. Shao,[42,52] C. P. Shen,[2] P. X. Shen,[34] X. Y. Shen,[1,46] H. Y. Sheng,[1] X. Shi,[1,42] J. J. Song,[36] W. M. Song,[36] X. Y. Song,[1] S. Sosio,[55a,55c] C. Sowa,[4] S. Spataro,[55a,55c] G. X. Sun,[1] J. F. Sun,[16] L. Sun,[57] S. S. Sun,[1,46] X. H. Sun,[1] Y. J. Sun,[42,52] Y. K. Sun,[42,52] Y. Z. Sun,[1] Z. J. Sun,[1,42] Z. T. Sun,[1] Y. T. Tan,[42,52] C. J. Tang,[39] G. Y. Tang,[1] X. Tang,[1] I. Tapan,[45c] M. Tiemens,[29] B. Tsednee,[25] I. Uman,[45d] B. Wang,[1] B. L. Wang,[46] C. W. Wang,[33] D. Wang,[35] D. Y. Wang,[35] Dan Wang,[46] K. Wang,[1,42] L. L. Wang,[1] L. S. Wang,[1] M. Wang,[36] Meng Wang,[1,46] P. Wang,[1] P. L. Wang,[1] W. P. Wang,[42,52] X. F. Wang,[44] Y. Wang,[42,52] Y. F. Wang,[1] Z. Wang,[1,42] Z. G. Wang,[1,42] Z. Y. Wang,[1] Zongyuan Wang,[1,46] T. Weber,[4] D. H. Wei,[12] P. Weidenkaff,[26] S. P. Wen,[1] U. Wiedner,[4] M. Wolke,[56] L. H. Wu,[1] L. J. Wu,[1,46] Z. Wu,[1,42] L. Xia,[42,52] X. Xia,[36] Y. Xia,[20] D. Xiao,[1] Y. J. Xiao,[1,46] Z. J. Xiao,[32] Y. G. Xie,[1,42] Y. H. Xie,[6] X. A. Xiong,[1,46] Q. L. Xiu,[1,42] G. F. Xu,[1] J. J. Xu,[1,46] L. Xu,[1] Q. J. Xu,[14] Q. N. Xu,[46] X. P. Xu,[40] F. Yan,[53] L. Yan,[55a,55c] W. B. Yan,[42,52] W. C. Yan,[2] Y. H. Yan,[20] H. J. Yang,[37,h] H. X. Yang,[1] L. Yang,[57] R. X. Yang,[42,52] Y. H. Yang,[33] Y. X. Yang,[12] Yifan Yang,[1,46] Z. Q. Yang,[20] M. Ye,[1,42] M. H. Ye,[7] J. H. Yin,[1] Z. Y. You,[43] B. X. Yu,[1] C. X. Yu,[34] J. S. Yu,[30] J. S. Yu,[20] C. Z. Yuan,[1,46] Y. Yuan,[1] A. Yuncu,[45b,a] A. A. Zafar,[54] Y. Zeng,[20] B. X. Zhang,[1] B. Y. Zhang,[1,42] C. C. Zhang,[1] D. H. Zhang,[1] H. H. Zhang,[43] H. Y. Zhang,[1,42] J. Zhang,[1,46] J. L. Zhang,[58] J. Q. Zhang,[4] J. W. Zhang,[1] J. Y. Zhang,[1] J. Z. Zhang,[1,46] K. Zhang,[1,46] L. Zhang,[44] S. F. Zhang,[33] T. J. Zhang,[37,h] X. Y. Zhang,[36] Y. Zhang,[42,52] Y. H. Zhang,[1,42] Y. T. Zhang,[42,52] Yang Zhang,[1] Yao Zhang,[1] Yu Zhang,[46] Z. H. Zhang,[6] Z. P. Zhang,[52] Z. Y. Zhang,[57] G. Zhao,[1] J. W. Zhao,[1,42] J. Y. Zhao,[1,46] J. Z. Zhao,[1,42] Lei Zhao,[42,52] Ling Zhao,[1] M. G. Zhao,[34] Q. Zhao,[1] S. J. Zhao,[60] T. C. Zhao,[1] Y. B. Zhao,[1,42] Z. G. Zhao,[42,52] A. Zhemchugov,[27,b] B. Zheng,[53] J. P. Zheng,[1,42] W. J. Zheng,[36] Y. H. Zheng,[46] B. Zhong,[32] L. Zhou,[1,42] Q. Zhou,[1,46] X. Zhou,[57] X. K. Zhou,[42,52] X. R. Zhou,[42,52] X. Y. Zhou,[1] Xiaoyu Zhou,[20] Xu Zhou,[20] A. N. Zhu,[1,46] J. Zhu,[34] J. Zhu,[43]

K. Zhu,[1] K. J. Zhu,[1] S. Zhu,[1] S. H. Zhu,[51] X. L. Zhu,[44] Y. C. Zhu,[42,52] Y. S. Zhu,[1,46] Z. A. Zhu,[1,46] J. Zhuang,[1,42] B. S. Zou,[1] and J. H. Zou[1]

(BESIII Collaboration)

[1]*Institute of High Energy Physics, Beijing 100049, People's Republic of China*
[2]*Beihang University, Beijing 100191, People's Republic of China*
[3]*Beijing Institute of Petrochemical Technology, Beijing 102617, People's Republic of China*
[4]*Bochum Ruhr-University, D-44780 Bochum, Germany*
[5]*Carnegie Mellon University, Pittsburgh, Pennsylvania 15213, USA*
[6]*Central China Normal University, Wuhan 430079, People's Republic of China*
[7]*China Center of Advanced Science and Technology, Beijing 100190, People's Republic of China*
[8]*COMSATS Institute of Information Technology, Lahore, Defence Road, Off Raiwind Road, 54000 Lahore, Pakistan*
[9]*Fudan University, Shanghai 200443, People's Republic of China*
[10]*G.I. Budker Institute of Nuclear Physics SB RAS (BINP), Novosibirsk 630090, Russia*
[11]*GSI Helmholtzcentre for Heavy Ion Research GmbH, D-64291 Darmstadt, Germany*
[12]*Guangxi Normal University, Guilin 541004, People's Republic of China*
[13]*Guangxi University, Nanning 530004, People's Republic of China*
[14]*Hangzhou Normal University, Hangzhou 310036, People's Republic of China*
[15]*Helmholtz Institute Mainz, Johann-Joachim-Becher-Weg 45, D-55099 Mainz, Germany*
[16]*Henan Normal University, Xinxiang 453007, People's Republic of China*
[17]*Henan University of Science and Technology, Luoyang 471003, People's Republic of China*
[18]*Huangshan College, Huangshan 245000, People's Republic of China*
[19]*Hunan Normal University, Changsha 410081, People's Republic of China*
[20]*Hunan University, Changsha 410082, People's Republic of China*
[21]*Indian Institute of Technology Madras, Chennai 600036, India*
[22]*Indiana University, Bloomington, Indiana 47405, USA*
[23a]*INFN Laboratori Nazionali di Frascati, I-00044 Frascati, Italy*
[23b]*INFN and University of Perugia, I-06100 Perugia, Italy*
[24a]*INFN Sezione di Ferrara, I-44122 Ferrara, Italy*
[24b]*University of Ferrara, I-44122 Ferrara, Italy*
[25]*Institute of Physics and Technology, Peace Ave. 54B, Ulaanbaatar 13330, Mongolia*
[26]*Johannes Gutenberg University of Mainz, Johann-Joachim-Becher-Weg 45, D-55099 Mainz, Germany*
[27]*Joint Institute for Nuclear Research, 141980 Dubna, Moscow region, Russia*
[28]*Justus-Liebig-Universitaet Giessen, II. Physikalisches Institut, Heinrich-Buff-Ring 16, D-35392 Giessen, Germany*
[29]*KVI-CART, University of Groningen, NL-9747 AA Groningen, The Netherlands*
[30]*Lanzhou University, Lanzhou 730000, People's Republic of China*
[31]*Liaoning University, Shenyang 110036, People's Republic of China*
[32]*Nanjing Normal University, Nanjing 210023, People's Republic of China*
[33]*Nanjing University, Nanjing 210093, People's Republic of China*
[34]*Nankai University, Tianjin 300071, People's Republic of China*
[35]*Peking University, Beijing 100871, People's Republic of China*
[36]*Shandong University, Jinan 250100, People's Republic of China*
[37]*Shanghai Jiao Tong University, Shanghai 200240, People's Republic of China*
[38]*Shanxi University, Taiyuan 030006, People's Republic of China*
[39]*Sichuan University, Chengdu 610064, People's Republic of China*
[40]*Soochow University, Suzhou 215006, People's Republic of China*
[41]*Southeast University, Nanjing 211100, People's Republic of China*
[42]*State Key Laboratory of Particle Detection and Electronics, Beijing 100049, Hefei 230026, People's Republic of China*
[43]*Sun Yat-Sen University, Guangzhou 510275, People's Republic of China*
[44]*Tsinghua University, Beijing 100084, People's Republic of China*
[45a]*Ankara University, 06100 Tandogan, Ankara, Turkey*
[45b]*Istanbul Bilgi University, 34060 Eyup, Istanbul, Turkey*
[45c]*Uludag University, 16059 Bursa, Turkey*
[45d]*Near East University, Nicosia, North Cyprus, Mersin 10, Turkey*
[46]*University of Chinese Academy of Sciences, Beijing 100049, People's Republic of China*
[47]*University of Hawaii, Honolulu, Hawaii 96822, USA*

[48]University of Jinan, Jinan 250022, People's Republic of China
[49]University of Minnesota, Minneapolis, Minnesota 55455, USA
[50]University of Muenster, Wilhelm-Klemm-Str. 9, 48149 Muenster, Germany
[51]University of Science and Technology Liaoning, Anshan 114051, People's Republic of China
[52]University of Science and Technology of China, Hefei 230026, People's Republic of China
[53]University of South China, Hengyang 421001, People's Republic of China
[54]University of the Punjab, 54590 Lahore, Pakistan
[55a]University of Turin, I-10125 Turin, Italy
[55b]University of Eastern Piedmont, I-15121 Alessandria, Italy
[55c]INFN, I-10125 Turin, Italy
[56]Uppsala University, Box 516, SE-75120 Uppsala, Sweden
[57]Wuhan University, Wuhan 430072, People's Republic of China
[58]Xinyang Normal University, Xinyang 464000, People's Republic of China
[59]Zhejiang University, Hangzhou 310027, People's Republic of China
[60]Zhengzhou University, Zhengzhou 450001, People's Republic of China

(Received 23 October 2018; published 31 January 2019)

Decays $\chi_{cJ}(J=0,1,2)\to\omega\phi$ are studied using $(448.1\pm2.9)\times10^6\psi(3686)$ events collected with the BESIII detector in 2009 and 2012. In addition to the previously established $\chi_{c0}\to\omega\phi$, the first observation of $\chi_{c1}\to\omega\phi$ is reported in this paper. The measured product branching fractions are $\mathcal{B}(\psi(3686)\to\gamma\chi_{c0})\times\mathcal{B}(\chi_{c0}\to\omega\phi)=(13.83\pm0.70\pm1.01)\times10^{-6}$ and $\mathcal{B}(\psi(3686)\to\gamma\chi_{c1})\times\mathcal{B}(\chi_{c1}\to\omega\phi)=(2.67\pm0.31\pm0.27)\times10^{-6}$, and the absolute branching fractions are $\mathcal{B}(\chi_{c0}\to\omega\phi)=(13.84\pm0.70\pm1.08)\times10^{-5}$ and $\mathcal{B}(\chi_{c1}\to\omega\phi)=(2.80\pm0.32\pm0.30)\times10^{-5}$. We also find strong evidence for $\chi_{c2}\to\omega\phi$ with a statistical significance of 4.8σ, and the corresponding product and absolute branching fractions are measured to be $\mathcal{B}(\psi(3686)\to\gamma\chi_{c2})\times\mathcal{B}(\chi_{c2}\to\omega\phi)=(0.91\pm0.23\pm0.12)\times10^{-6}$ and $\mathcal{B}(\chi_{c2}\to\omega\phi)=(1.00\pm0.25\pm0.14)\times10^{-5}$. Here, the first errors are statistical and the second ones systematic.

DOI: 10.1103/PhysRevD.99.012015

I. INTRODUCTION

The lowest triplet P-wave states of charmonium (the $c\bar{c}$ bound state), $\chi_{cJ}(1P)$, with quantum numbers $I^GJ^{PC}=0^+J^{++}$ and $J=0$, 1, and 2, can be found abundantly in the electromagnetic decays $\psi(3686)\to\gamma\chi_{cJ}$ with an approximate branching fraction of 30% [1]. The $\psi(3686)$ meson can be directly produced at the e^+e^- colliders, such as the BEPCII [2], where the χ_{cJ} mesons are easily accessible by the electromagnetic decays $\psi(3686)\to\gamma\chi_{cJ}$.

The hadronic χ_{cJ} decays are important probes of the strong force dynamics. First of all, the mass of the c quark (~1.5 GeV/c^2) is well known between the perturbative and nonperturbative QCD domains in theoretical calculations. Due to the complexity and entanglement of the long- and short-distance contributions, large theoretical uncertainties of branching ratios for the $\chi_{cJ}\to VV$ decays are known [3–9]. (In this paper, the symbol of V denotes the ω and ϕ mesons). The hadronic χ_{cJ} decays provide a prospective laboratory to limit theoretical parameters and test various phenomenological models. Second, the χ_{cJ} mesons have the same quantum numbers J^{PC} as some glueballs and hybrids, although none of the glueball and hybrid states has been seen until now [10]. The hadronic $\chi_{cJ}\to VV$ decays are ideal objects to exploit the glueball-$q\bar{q}$ mixing and the quark-gluon coupling of the strong

*Corresponding author.
jiqingping@htu.edu.cn
[a]Also at Bogazici University, 34342 Istanbul, Turkey.
[b]Also at the Moscow Institute of Physics and Technology, Moscow 141700, Russia.
[c]Also at the Functional Electronics Laboratory, Tomsk State University, Tomsk 634050, Russia.
[d]Also at the Novosibirsk State University, Novosibirsk 630090, Russia.
[e]Also at the NRC "Kurchatov Institute", PNPI, Gatchina 188300, Russia.
[f]Also at Istanbul Arel University, 34295 Istanbul, Turkey.
[g]Also at Goethe University Frankfurt, 60323 Frankfurt am Main, Germany.
[h]Also at Key Laboratory for Particle Physics, Astrophysics and Cosmology, Ministry of Education; Shanghai Key Laboratory for Particle Physics and Cosmology; Institute of Nuclear and Particle Physics, Shanghai 200240, People's Republic of China.
[i]Government College Women University, Sialkot 51310, Punjab, Pakistan.
[j]Key Laboratory of Nuclear Physics and Ion-beam Application (MOE) and Institute of Modern Physics, Fudan University, Shanghai 200443, People's Republic of China.

interactions at the relatively low energies. Third, the χ_{cJ} mesons are below the open-charm threshold. Most of the hadronic χ_{cJ} decay modes are suppressed by the Okubo-Zweig-Iizuka (OZI) rule [11]. It is shown in the previous theoretical researches that the contributions from the intermediate glueballs or hadronic loops can scuttle the OZI rule in the $\chi_{cJ} \to VV$ decays [12–15], and avoid the so-called helicity selection (HS) rule (also called the "naturalness" which is defined as $\sigma = (-1)^S P$ [16], where S and P are respectively the spin and parity of the particle.) in the $\chi_{c1} \to VV$ decays [8,9].

The χ_{cJ}, ϕ and ω mesons differ from each other in their quark components according to the quark model assignments. This fact causes the $\chi_{cJ} \to \omega\phi$ decay modes to be doubly OZI (DOZI) suppressed and results in the branching fractions for the $\chi_{cJ} \to \omega\phi$ decays much less than those for the singly OZI-suppressed $\chi_{cJ} \to \omega\omega$, $\phi\phi$ decays [1,17]. In reality, ω and ϕ are not ideal mixtures of the flavor SU(3) octet and singlet [18], which would provide a source that violates the DOZI-suppressed rule for $\chi_{c1} \to \omega\phi$. The DOZI-suppressed $\chi_{cJ} \to \omega\phi$ decays have been observed based on the 106×10^6 $\psi(3686)$ events accumulated with the BESIII detector in 2009, with significances of 10σ, 4.1σ and 1.5σ for the χ_{c0}, χ_{c1} and χ_{c2} decays, respectively [17].

In this paper, the $\chi_{cJ} \to \omega\phi$ decays will be reinvestigated via the radiative transitions $\psi(3686) \to \gamma\chi_{cJ}$ with combined experimental data, i.e., $(448.1 \pm 2.9) \times 10^6$ $\psi(3686)$ events collected with the BESIII detector during 2009 and 2012 [19].

II. BESIII DETECTOR AND MONTE CARLO SIMULATION

The BESIII detector operating at the BEPCII collider is described in detail in Ref. [2]. The detector is cylindrically symmetric and covers 93% of 4π solid angle. It consists of the following four subdetectors: a 43-layer main drift chamber (MDC), which is used to determine momentum of the charged tracks with a resolution of 0.5% at 1 GeV/c in the axial magnetic field of 1 T; a plastic scintillator time-of-flight system (TOF), with a time resolution of 80 ps (110 ps) in the barrel (end caps); an electromagnetic calorimeter (EMC) consisting of 6240 CsI(Tl) crystals, with photon energy resolution at 1 GeV of 2.5% (5%) in the barrel (end caps); and a muon counter consisting of 9 (8) layers of resistive plate chambers in the barrel (end caps), with position resolution of 2 cm.

The GEANT4-based [20,21] Monte Carlo (MC) simulation software BOOST [22] includes the geometry and material description of the BESIII detectors, the detector response and digitization models, as well as a database that keeps track of the running conditions and the detector performance. MC samples are used to optimize the selection criteria, evaluate the signal efficiency, and estimate physics backgrounds. An inclusive MC sample of $\psi(3686)$ events is used for the background studies. The $\psi(3686)$ resonance is produced by the event generator KKMC [23], where the initial state radiation is included, and the decays are simulated by EVTGEN [24] with known branching fractions taken from Ref. [1], while the unmeasured decays are generated according to LUNDCHARM [25]. The signal is simulated with the decay $\psi(3686) \to \gamma\chi_{cJ}$ generated assuming an electric-pole ($E1$) transition. The decay $\chi_{cJ} \to \omega\phi$ is generated using HELAMP [24], the helicity amplitude model where the angular correlation between ω decay and ϕ decay has been considered. Ref. [17] shows that the model describes the experimental angular distribution well. We assume $\chi_{cJ} \to \omega\phi$ and $\chi_{cJ} \to \phi\phi$ have the same helicity amplitudes with the same HELAMP parameters. In addition, χ_{cJ} states are simulated using a relativistic Breit-Wigner incorporated within the helicity amplitudes in the EVTGEN package [24]. The background decays $\chi_{cJ} \to \omega K^+K^-$, $\phi\pi^+\pi^-\pi^0$, and the nonresonant decay $\chi_{cJ} \to K^+K^-\pi^+\pi^-\pi^0$ are generated using the phase space model.

III. EVENT SELECTION

In this analysis, the ϕ mesons are reconstructed by K^+K^-, while ω by $\pi^+\pi^-\pi^0$. Event candidates are required to have four well-reconstructed tracks from charged particles with zero net charge, and at least three good photon candidates.

A charged track reconstructed from MDC hits should have the polar angle, θ, $|\cos\theta| < 0.93$ and pass within ± 10 cm of the interaction point along the beam direction and within 1 cm in the plane perpendicular to the beam. To separate $K^\pm$ from $\pi^\pm$, we require that at least one track is identified as a kaon using dE/dx and TOF information. If the identified kaon has a positive (negative) charge, the second kaon is found by searching for a combination that minimizes $|M_{K^+K^-} - M_\phi|$, among all identified kaons and the negative (positive) charged tracks, where $M_{K^+K^-}$ is the invariant mass of the identified kaon and an unidentified track with kaon mass hypothesis, and M_ϕ is the nominal ϕ mass [1]. The remaining two charged tracks are assumed to be pions.

The photon energy deposit is required to be at least 25 MeV in the barrel region of the EMC ($|\cos\theta| < 0.80$) or 50 MeV in the EMC end caps ($0.86 < |\cos\theta| < 0.92$). To suppress electronic noise and energy deposits unrelated to the event, the EMC time t of the photon candidates must be in coincidence with collision events within the range $0 \le t \le 700$ ns. At least three photons are required in an event.

In order to improve the mass resolution, a four-constraint (4C) kinematic fit is performed by assuming energy-momentum conservation for the $\psi(3686) \to 3\gamma K^+K^-\pi^+\pi^-$ process. If the number of photons is larger than three, then looping all $3\gamma K^+K^-\pi^+\pi^-$ combinations and the one with the smallest χ^2_{4C} is chosen. The event is kept for further analysis if $\chi^2_{4C}(3\gamma K^+K^-\pi^+\pi^-) < 60$, which is obtained by optimizing the figure of merit (FOM) $S/\sqrt{S+B}$, where S and B

are the numbers of MC simulated signal and background events, respectively. In addition, $\chi^2_{4C}(3\gamma K^+K^-\pi^+\pi^-) < \chi^2_{4C}(4\gamma K^+K^-\pi^+\pi^-)$ is applied to suppress the background with an extra photon in the final state.

A further requirement of $|M^{\rm recoil}_{\pi^+\pi^-} - M_{J/\psi}| > 8$ MeV/c^2 obtained by optimizing FOM, is applied to suppress the $\psi(3686) \to \pi^+\pi^- J/\psi$ background, where the $M^{\rm recoil}_{\pi^+\pi^-}$ is the recoil mass for the $\pi^+\pi^-$ system, and $M_{J/\psi}$ is the nominal mass of J/ψ [1].

The π^0 candidates are selected from the three $\gamma\gamma$ combinations as the pair with the minimum $|M_{\gamma\gamma} - M_{\pi^0}|$, where M_{π^0} is the nominal π^0 mass [1]. Figure 1(a) shows the plot of the K^+K^- vs $\pi^+\pi^-\pi^0$ invariant mass for the selected events in the χ_{cJ} signal region ($[3.3, 3.6]$ GeV/c^2), and a clear accumulation at the ω and ϕ masses is observed. The bottom-central square $|M_{\pi^+\pi^-\pi^0} - M_\omega| < 0.05$ GeV/c^2 and $|M_{K^+K^-} - M_\phi| < 0.015$ GeV/c^2 obtained by optimizing FOM, is taken as the $\omega\phi$ signal region (labeled as D), and the five squares around the signal region are taken as the sideband regions (labeled as A, B and C), where $M_{\pi^+\pi^-\pi^0}(M_{K^+K^-})$ is the invariant mass of $\pi^+\pi^-\pi^0(K^+K^-)$. The $M_{K^+K^-}$ distribution with $M_{\pi^+\pi^-\pi^0}$ in the ω signal region in Fig. 1(b) shows a clear ϕ peak. Correspondingly, the

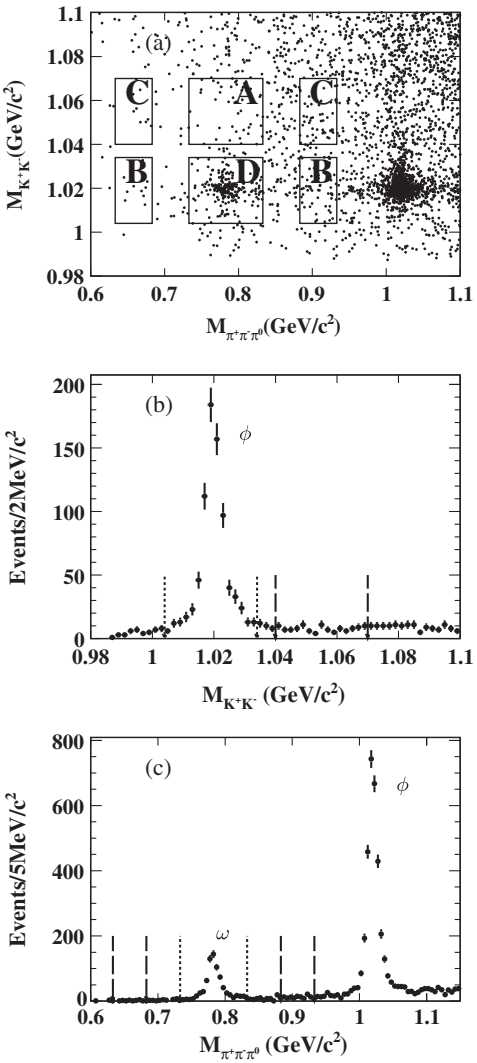

FIG. 1. (a) Scatter plot of $M_{K^+K^-}$ vs $M_{\pi^+\pi^-\pi^0}$ for events within the χ_{cJ} mass region. The boxes indicate the sideband regions (labeled as A, B, and C) and signal region (labeled as D). (b) and (c) are the one-dimensional projection of the system recoiling against selected ω and ϕ candidates, respectively. The short-dashed arrows show the signal regions while long-dashed arrows show the sideband regions.

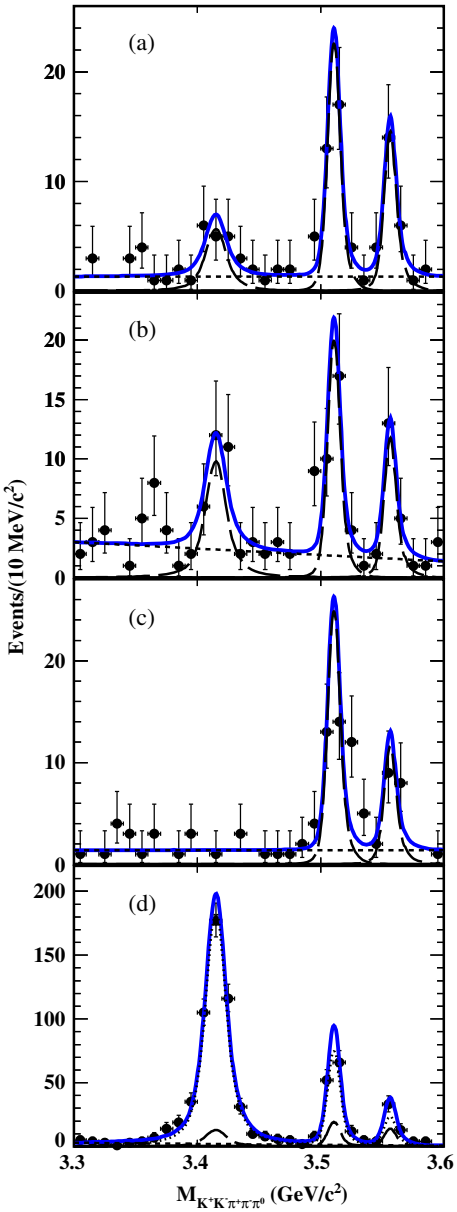

FIG. 2. Simultaneous fit to the $M_{K^+K^-\pi^+\pi^-\pi^0}$ distributions in the sidebands (A, B, and C) and the signal (D) regions. The dots with error bars are data, the solid lines are the fit results, and the dotted lines represent the signal components. The long-dashed line is background normalized using the simultaneous fit to the $\omega\phi$ sidebands, and the short-dashed line is the remaining background.

$M_{\pi^+\pi^-\pi^0}$ distribution with $M_{K^+K^-}$ within the ϕ signal region, as shown in Fig. 1(c), indicates clear ω and ϕ peaks. The latter is from the decay $\chi_{cJ} \to \phi\phi \to K^+K^-\pi^+\pi^-\pi^0$. Figure 2 shows the invariant mass spectrum $M_{K^+K^-\pi^+\pi^-\pi^0}$ for events in the $\omega\phi$ sideband regions (subfigures labeled A, B, and C) and the signal region (subfigure labeled D) with clear χ_{cJ} peaks in all plots.

Analysis of the $\psi(3686)$ inclusive MC sample indicates that the peaking background in the χ_{cJ} signal region can be described by the sideband events. The data collected at $\sqrt{s} = 3.65$ GeV with an integrated luminosity of approximately $1/15$ of the $\psi(3686)$ data are used to investigate nonresonant continuum background. After the same event selection criteria are applied, only a few events survive, and they do not have any obvious enhancements in the χ_{cJ} mass region.

IV. SIGNAL EXTRACTION

The number of the $\chi_{cJ} \to \omega\phi$ events is determined by fitting the $M_{K^+K^-\pi^+\pi^-\pi^0}$ distributions within the $\omega\phi$ signal region [labeled as D in Fig. 1(a)]. The signal is described by the MC simulated shape convolved with a Gaussian function, which is used to account for the difference in the χ_{cJ} mass and resolution between data and MC simulation. The parameters of the Gaussian function are obtained using the sample $\psi(3686) \to \gamma\chi_{cJ} \to \gamma\phi\phi \to \gamma\pi^+\pi^-\pi^0K^+K^-$.

The peaking backgrounds from the $\chi_{cJ} \to \omega K^+K^-$, $\phi\pi^+\pi^-\pi^0$, and the nonresonant $K^+K^-\pi^+\pi^-\pi^0$ background are estimated using the sideband regions labeled A, B, and C in Fig. 1(a). The total peaking background contribution, $N_{\rm bkg}$, is the sum calculated as

$$N_{\rm bkg} = N_{\rm bkg}^{\omega K^+K^-} + N_{\rm bkg}^{\phi\pi^+\pi^-\pi^0} + N_{\rm bkg}^{\rm n-r}, \quad (1)$$

where $N_{\rm bkg}^{\omega K^+K^-}, N_{\rm bkg}^{\phi\pi^+\pi^-\pi^0}$, and $N_{\rm bkg}^{\rm n-r}$ are numbers of the aforementioned peaking background contributions. The contributions are determined using the following equations:

$$N_{\rm bkg}^{\omega K^+K^-} = (N_{\rm A} - N_{\rm C}\cdot f_{\rm C\to A})\cdot f_{\rm A\to D}, \quad (2)$$

$$N_{\rm bkg}^{\phi\pi^+\pi^-\pi^0} = (N_{\rm B} - N_{\rm C}\cdot f_{\rm C\to B})\cdot f_{\rm B\to D}, \quad (3)$$

$$N_{\rm bkg}^{\rm n-r} = N_{\rm C}\cdot f_{\rm C\to D}, \quad (4)$$

where $N_{\rm A}$, $N_{\rm B}$, and $N_{\rm C}$ are the numbers of the fitted χ_{cJ} events in the A, B, and C regions, respectively; $f_{\rm C\to A}$, $f_{\rm C\to B}$, $f_{\rm C\to D}$, $f_{\rm A\to D}$, and $f_{\rm B\to D}$ are the relative scaling factors for the different regions. The factors are estimated using the corresponding MC simulation of $\chi_{cJ} \to K^+K^-\pi^+\pi^-\pi^0$, ωK^+K^-, and $\phi\pi^+\pi^-\pi^0$. For example, $f_{\rm A\to D}$ is the ratio of the $\chi_{cJ} \to \omega K^+K^-$ yields between the D and A regions.

We perform a simultaneous unbinned maximum likelihood fit to the $M_{K^+K^-\pi^+\pi^-\pi^0}$ distributions in the signal and sideband regions. The result of the fit is shown in Fig. 2. The parameters of the Gaussian functions accounting for the difference between data and MC simulation are assumed to be the same for the signal and sidebands. The shape of the distributions outside the χ_{cJ} peaks is described by a polynomial function. The statistical significance of the $\chi_{c1}(\chi_{c2})$ signal is determined by comparing the $-2\ln\mathcal{L}$ value with the one from the fit without the $\chi_{c1}(\chi_{c2})$ signal component, and considering the change in the number of degrees of freedom. The results are 12.3σ and 4.8σ for χ_{c1} and χ_{c2}, respectively. The extracted numbers of the $\chi_{cJ} \to \omega\phi$ events are given in Table I.

The product branching fractions, $\mathcal{B}(\psi(3686) \to \gamma\chi_{cJ})\times \mathcal{B}(\chi_{cJ} \to \omega\phi) = \mathcal{B}_1 \times \mathcal{B}_2$, are calculated as

$$\mathcal{B}_1 \times \mathcal{B}_2 = \frac{N_{\rm obs}^{\chi_{cJ}}}{N_{\psi(3686)}\cdot\mathcal{B}(\omega)\cdot\mathcal{B}(\phi)\cdot\mathcal{B}(\pi^0)\cdot\epsilon}, \quad (5)$$

where $N_{\psi(3686)}$ is the number of $\psi(3686)$ events, $\mathcal{B}(\omega)$, $\mathcal{B}(\phi)$, and $\mathcal{B}(\pi^0)$ are the branching fractions of $\omega \to \pi^+\pi^-\pi^0$, $\phi \to K^+K^-$, and $\pi^0 \to \gamma\gamma$, respectively [1]. The corresponding detection efficiencies, ϵ, are obtained from the MC simulations. The results for the product branching fractions are listed in Table I.

By using the world average values of $\mathcal{B}(\psi(3686) \to \gamma\chi_{cJ})$, the absolute branching fractions of $\chi_{cJ} \to \omega\phi$ are determined and also listed in Table I.

V. SYSTEMATIC UNCERTAINTIES

The contribution of systematic effects on the product branching fractions from various sources is described in the following:

(1) The tracking efficiency for π and K is investigated using control samples of $J/\psi \to \rho\pi$ [17] and $\psi(3686) \to \pi^+\pi^-K^+K^-$, respectively. The difference in the efficiency for the track reconstruction between data and MC simulation is 1.0% per pion

TABLE I. Number of signal events ($N_{\rm obs}^{\chi_{cJ}}$), detection efficiency (ϵ), the product branching fraction $\mathcal{B}_1 \times \mathcal{B}_2 = \mathcal{B}(\psi(3686) \to \gamma\chi_{cJ}) \times \mathcal{B}(\chi_{cJ} \to \omega\phi)$, and the absolute branching fraction $\mathcal{B}(\chi_{cJ} \to \omega\phi)$. Here, the first uncertainty is statistical and the second systematic.

Mode	$N_{\rm obs}^{\chi_{cJ}}$	$\epsilon(\%)$	$\mathcal{B}_1 \times \mathcal{B}_2$	$\mathcal{B}(\chi_{cJ} \to \omega\phi)$
$\chi_{c0} \to \omega\phi$	486.3 ± 24.5	17.99 ± 0.06	$(13.83 \pm 0.70 \pm 1.01) \times 10^{-6}$	$(13.84 \pm 0.70 \pm 1.08) \times 10^{-5}$
$\chi_{c1} \to \omega\phi$	104.7 ± 12.1	20.04 ± 0.06	$(2.67 \pm 0.31 \pm 0.27) \times 10^{-6}$	$(2.80 \pm 0.32 \pm 0.30) \times 10^{-5}$
$\chi_{c2} \to \omega\phi$	32.9 ± 8.3	18.47 ± 0.06	$(0.91 \pm 0.23 \pm 0.12) \times 10^{-6}$	$(1.00 \pm 0.25 \pm 0.14) \times 10^{-5}$

and per kaon. Assuming they are all correlated, the uncertainty due to tracking efficiency is 4%.

(2) The particle identification (PID) efficiency for kaons is investigated with control samples of $J/\psi \to K^*(892)^0 K_S^0 + \text{c.c.}$, and the systematic uncertainty is determined to be 1% per kaon track [17]. In this analysis, only one of the two charged tracks is required to be identified as kaon. The bias on one of the two tracks being a kaon track will be much smaller than 1%. Therefore, the uncertainty due to PID efficiency is negligible.

(3) The uncertainty of the photon reconstruction efficiency is studied using $J/\psi \to \rho\pi$ [26]. The difference between data and MC simulation is found to be 1.0% per photon, and the value 3% is taken as the systematic uncertainty.

(4) The uncertainty of MC generator comes from modeling $\psi(3686) \to \gamma\chi_{c1,2}$ and $\chi_{cJ} \to \omega\phi$ in MC simulation.

The uncertainty of assuming $\psi(3686) \to \gamma\chi_{c1,2}$ as pure E1 transition is studied by taking the higher-order multiple amplitudes contribution [27] into account in the MC simulation. The resulting efficiency difference of 0.9% for χ_{c1}, and 0.5% for χ_{c2}, are taken as this systematic uncertainty. The uncertainty of modeling $\chi_{cJ} \to \omega\phi$ is studied by changing the model from HELAMP to a pure phase space distribution. The resulting efficiency difference of 4.1% for χ_{c0}, 5.6% for χ_{c1}, and 1.3% for χ_{c2}, are taken as this systematic uncertainty.

The total systematic uncertainties of the MC generator are obtained as 4.1% for χ_{c0}, 5.7% for χ_{c1}, and 1.4% for χ_{c2} by summing all individual contributions in quadrature, assuming two sources to be independent.

(5) The uncertainty related to the π^0 mass window is studied by fitting the π^0 mass distribution of data and signal MC for the control sample $\psi(3686) \to \pi^+\pi^-\pi^0$. We obtain the π^0 detection efficiency, which is the ratio of the number of π^0 events selected with and without the π^0 mass window requirement, determined by integrating the fitted signal shape. The difference in the efficiency between data and MC simulation is 0.8%.

(6) The uncertainty related to the $M^{\text{recoil}}_{\pi^+\pi^-}$ mass window requirement is studied with the control sample $\psi(3686) \to \pi^+\pi^- J/\psi, J/\psi \to \mu^+\mu^-$. We obtain the $M^{\text{recoil}}_{\pi^+\pi^-}$ detection efficiency, which is the ratio of the number of events with and without the $M^{\text{recoil}}_{\pi^+\pi^-}$ mass window. The difference in the efficiency between data and MC simulation is 0.4%.

(7) The systematic uncertainties associated with the 4C kinematic fit are studied with the track helix parameter correction method, as described in Ref. [28]. In the standard analysis, these corrections are applied. The difference of the MC signal efficiencies with the uncorrected track parameters are 1.5%, 1.9%, and 2.3% for χ_{c0}, χ_{c1}, and χ_{c2} decays, respectively. These values are taken as the uncertainties associated with the 4C kinematic fit.

(8) The uncertainty related to the fitting comes from the fit range, ω and ϕ mass windows, sideband regions, and fitting function (including resolution and remaining backgrounds shape).

(a) The uncertainty due to the fit range is estimated by changing the range by ± 5 MeV/c^2 in the mass spectrum, since the nonresonant $K^+K^-\pi^+\pi^-\pi^0$ background shape is quite smooth according to the topology analysis with the inclusive MC sample. The largest differences for the branching ratios are 1.0% for χ_{c0}, 3.0% for χ_{c1}, and 10.0% for χ_{c2}. These numbers are assigned as the corresponding systematic uncertainties.

(b) The uncertainties associated with the ϕ and ω mass windows are estimated using two control samples, $\psi(3686) \to \gamma\chi_{cJ}, \chi_{cJ} \to \phi\phi \to (K^+K^-)(\pi^+\pi^-\pi^0)$, and $\psi(3686) \to \gamma\chi_{cJ}, \chi_{cJ} \to \omega\omega \to 2(\pi^+\pi^-\pi^0)$, respectively. The efficiency for the $\omega(\phi)$ selection is obtained from the comparison of the ω (ϕ) yields determined from the $\pi^+\pi^-\pi^0$ (K^+K^-) mass spectrum with and without the ω (ϕ) selection requirement. The difference in $\omega(\phi)$-selection efficiency between data and MC simulation, 1.9% (0.6%), is taken as the uncertainty of the $\omega(\phi)$-mass window.

(c) The uncertainty due to background estimates using the sidebands can be divided in two groups. One is due to the sideband ranges, the other is due to contributions of various intermediate states in $\chi_{cJ} \to K^+K^-\pi^+\pi^-\pi^0$ in the MC simulation used to extract the scaling factors. The former can be estimated by changing the sideband range. By changing the mass region of $M_{\pi^+\pi^-\pi^0}$ from [0.633,0.683]/[0.883,0.933] to [0.631,0.681]/[0.881,0.931]GeV/c^2, and the mass region of $M_{K^+K^-}$ from [1.04, 1.07] to [1.042, 1.072] GeV/c^2, the differences of $\chi_{c0,1,2}$ signal yields are 0.6%, 4.6%, and 5.1%, respectively. For the nonresonant $\chi_{cJ} \to K^+K^-\pi^+\pi^-\pi^0$, a phase space process was used. The experimental distributions indicate the contribution of the intermediate states involving $K^*(892)$: $\chi_{cJ} \to K^{*0}\bar{K}^{*0}\pi^0$ and $\chi_{cJ} \to K^{*+}K^-\pi^+\pi^- + \text{c.c.}$. The corresponding MC distributions are mixed with the phase space model according to the ratios estimated from the fits to data to recalculate the scale factors related to the region C. The differences of the $\chi_{c0,1,2}$ signal yields are 0.2%, 2.0%, and 4.2%, respectively. The resulting differences due to the two preceding effects are

TABLE II. Relative contributions to systematic uncertainties in measuring the product branching fraction of $\mathcal{B}_1 \times \mathcal{B}_2 = \mathcal{B}(\psi(3686) \to \gamma\chi_{cJ}) \times \mathcal{B}(\chi_{cJ} \to \omega\phi)$ (in units of %).

Source	χ_{c0}	χ_{c1}	χ_{c2}
Tracking efficiency	4.0	4.0	4.0
PID efficiency	Negligible	Negligible	Negligible
Photon efficiency	3.0	3.0	3.0
MC generator	4.1	5.7	1.4
π^0 mass window	0.8	0.8	0.8
$M^{\rm recoil}_{\pi^+\pi^-}$ mass window	0.4	0.4	0.4
Kinematic fit	1.5	1.9	2.3
Fit range	1.0	3.0	10.0
ω mass window	1.9	1.9	1.9
ϕ mass window	0.6	0.6	0.6
Sidebands	0.6	5.0	6.6
Resolution	Negligible	Negligible	Negligible
Remaining background shape	0.4	0.5	0.2
Intermediate state	1.3	1.3	1.3
$N_{\psi(3686)}$	0.6	0.6	0.6
Total	7.2	10.2	13.7

found to be 0.6%, 5.0%, and 6.6% for $\chi_{c0,1,2}$, respectively.

(d) The systematic effects from the detector resolution difference between data and MC simulation are studied with the control sample $\psi(3686) \to \gamma\chi_{cJ} \to \phi\phi \to K^+K^-\pi^+\pi^-\pi^0$. We change the difference by one standard deviation. No changes are found for the $\chi_{c0,1,2}$ signal yields and these systematic uncertainties are neglected.

(e) The uncertainty from the non-χ_{cJ} background is estimated by changing the polynomial from first to second order in fitting $M_{K^+K^-\pi^+\pi^-\pi^0}$ mass spectrum. The differences in the final results are 0.4%, 0.5%, and 0.2%, respectively.

(9) The systematic uncertainties due to the branching fractions of $\omega \to \pi^+\pi^-\pi^0$ and $\phi \to K^+K^-$ are 0.8% and 1.0%, respectively [1]. Therefore, the uncertainties of the final results are 1.3%.

(10) The number of $\psi(3686)$ events is estimated from the number of inclusive hadronic events, as described in Ref. [19]. The uncertainty of the total number of $\psi(3686)$ events is 0.6%.

Table II summarizes the systematic uncertainties and their sources for the product branching fractions. The total systematic uncertainties are obtained by summing all individual contributions in quadrature, assuming all sources to be independent. For the uncertainties of absolute branching fractions $\chi_{cJ} \to \omega\phi$, the uncertainty arising from $\psi(3686) \to \gamma\chi_{cJ}$ transition rate is added.

VI. RESULTS AND DISCUSSION

Using the data sample of $(448.1 \pm 2.9) \times 10^6$ $\psi(3686)$ events collected with the BESIII detector, we present the improved measurement of the doubly OZI-suppressed decays $\chi_{cJ} \to \omega\phi$. The decay $\chi_{c1} \to \omega\phi$ is observed for the first time with a 12.3σ statistical significance and the branching fraction of $\chi_{c0} \to \omega\phi$ is measured with improved precision. We also observe strong evidence for $\chi_{c2} \to \omega\phi$ at a statistical significance of 4.8σ. The product branching fractions, $\mathcal{B}(\psi(3686) \to \gamma\chi_{c0,1,2}) \times \mathcal{B}(\chi_{c0,1,2} \to \omega\phi)$, and the absolute branching fractions, $\mathcal{B}(\chi_{c0,1,2} \to \omega\phi)$, are determined as listed in Table I. In addition, using the branching fractions of $\chi_{c1} \to \omega\omega, \phi\phi$ from Ref. [17], the ratios $\mathcal{B}(\chi_{c1} \to \omega\phi)/\mathcal{B}(\chi_{c1} \to \omega\omega)$ and $\mathcal{B}(\chi_{c1} \to \omega\phi)/\mathcal{B}(\chi_{c1} \to \phi\phi)$ of $(4.67 \pm 0.78) \times 10^{-2}$ and $(5.60 \pm 1.01) \times 10^{-2}$ are obtained, respectively. Here, the common systematic uncertainties in the two measurements cancel in the ratio. These ratios are one order of magnitude larger than the theoretical predictions [9]. These measurements will be helpful in clarifying the influence of the long-distance contributions in this energy region, understanding the theoretical dilemma surrounding the OZI and HS rules, and checking mesonic loop contributions and the $\omega - \phi$ mixing effect.

ACKNOWLEDGMENTS

The BESIII Collaboration thanks the staff of BEPCII and the IHEP computing center for their strong support. This work is supported in part by the National Key Basic Research Program of China under Contract No. 2015CB856700; National Natural Science Foundation of China (NSFC) under Contracts No. 11335008, No. 11425524, No. 11625523, No. 11635010, No. 11735014, and No. 11605042; the Chinese Academy of Sciences (CAS) Large-Scale Scientific Facility Program; the CAS Center for Excellence in Particle Physics (CCEPP); Joint Large-Scale Scientific Facility Funds of the NSFC and CAS under Contracts No. U1632109, No. U1532257, No. U1532258, and No. U1732263; CAS Key Research Program of Frontier Sciences under Contracts No. QYZDJ-SSW-SLH003 and No. QYZDJ-SSW-SLH040; 100 Talents Program of CAS; CAS Open Research Program of Large Research Infrastructures under Contract No. 1G2017IHEPKFYJ01; INPAC and Shanghai Key Laboratory for Particle Physics and Cosmology; German Research Foundation DFG under Collaborative Research Center Contracts No. CRC 1044 and No. FOR 2359; Istituto Nazionale di Fisica Nucleare, Italy; Koninklijke Nederlandse Akademie van Wetenschappen (KNAW) under Contract No. 530-4CDP03; Ministry of Development of Turkey under Contract No. DPT2006K-120470; National Science and Technology Fund; The Swedish Research Council; U.S. Department of Energy under Contracts No. DE-FG02-05ER41374, No. DE-SC-0010118, No. DE-SC-0010504, and No. DE-SC-0012069; University of Groningen (RuG) and the Helmholtzzentrum fuer

Schwerionenforschung GmbH (GSI), Darmstadt; China Postdoctoral Science Foundation under Contract No. 2017M622347, Post-doctoral research start-up fees of Henan Province under Contract No. 2017SBH005 and Ph.D research start-up fees of Henan Normal University under Contract No. qd16164; Program for Innovative Research Team in University of Henan Province (Grant No. 19IRTSTHN018).

[1] C. Patrignani *et al.* (Particle Data Group), Review of particle physics, Chin. Phys. C **40**, 100001 (2016).
[2] M. Ablikim *et al.* (BESIII Collaboration), Design and construction of the BESIII detector, Nucl. Instrum. Methods Phys. Res., Sect. A **614**, 345 (2010).
[3] A. Luchinsky, Leading-twist contribution to $\chi_{c0,2} \to \omega\omega$ decays, Phys. At. Nucl. **70**, 53 (2007).
[4] V. V. Braguta, A. K. Likhoded, and A. V. Luchinsky, Observation potential for χ_b at the Fermilab Tevatron and CERN LHC, Phys. Rev. D **72**, 094018 (2005).
[5] H. Q. Zhou, R. G. Ping, and B. S. Zou, Mechanisms for $\chi_{cJ} \to \phi\phi$ decays, Phys. Lett. B **611**, 123 (2005).
[6] Q. Zhao, Coherent study of $\chi_{c0,2} \to VV, PP$ and SS, Phys. Rev. D **72**, 074001 (2005).
[7] Q. Zhao, $\chi_{c0,2}$ decay into light meson pairs and its implication of the scalar meson structures, Phys. Lett. B **659**, 221 (2008).
[8] X. H. Liu and Q. Zhao, Evasion of helicity selection rule in $\chi_{c1} \to VV$ and $\chi_{c2} \to VP$ via intermediate charmed meson loops, Phys. Rev. D **81**, 014017 (2010).
[9] D. Y. Chen, J. He, X. Q. Li, and X. Liu, Understanding the branching ratios of $\chi_{c1} \to \phi\phi, \omega\omega, \omega\phi$ observed at BES-III, Phys. Rev. D **81**, 074006 (2010).
[10] F. Giacosa, Modelling glueballs, EPJ Web Conf. **130**, 01009 (2016).
[11] S. Okubo, Phi meson and unitary symmetry model, Phys. Lett. **5**, 165 (1963); G. Zweig, An SU_3 model for strong interaction symmetry and its breaking, CERN Reports No. CERN-TH-401 and No. CERN-TH-412; J. Iizuka, A systematics, and phenomenology of meson family, Prog. Theor. Phys. Suppl. **37**, 21 (1966).
[12] P. Geiger and N. Isgur, When can hadronic loops scuttle the Okubo-Zweig-Iizuka rule?, Phys. Rev. D **47**, 5050 (1993).
[13] N. Isgur and H. B. Thacker, Origin of the Okubo-Zweig-Iizuka rule in QCD, Phys. Rev. D **64**, 094507 (2001).
[14] H. J. Lipkin and B. S. Zou, Comment on "When can hadronic loops scuttle the Okubo-Zweig-Iizuka rule?", Phys. Rev. D **53**, 6693 (1996).
[15] Q. Zhao, B. S. Zou, and Z. B. Ma, Glueball-Q anti-Q mixing and Okuba-Zweig-Iizuka rule violation in the hadronic decays of heavy quarkonia, Phys. Lett. B **631**, 22 (2005).
[16] V. Chernyak and A. Zhitnitsky, Exclusive decays of heavy mesons, Nucl. Phys. **B201**, 492 (1982).
[17] M. Ablikim *et al.* (BESIII Collaboration), Observation of χ_{c1} Decays into Vector Meson Pairs $\phi\phi$, $\omega\omega$, and $\omega\phi$, Phys. Rev. Lett. **107**, 092001 (2011).
[18] M. Benayoun, L. DelBuono, S. Eidelman, V. N. Ivanchenko, and H. B. O'Connell, Radiative decays, nonet symmetry, and SU(3) breaking, Phys. Rev. D **59**, 114027 (1999); M. Benayoun, L. DelBuono, and H. B. O'Connell, An effective approach to VMD at one loop order and the departures from ideal mixing for vector mesons, Eur. Phys. J. C **17**, 303 (2000); M. Benayoun, P. David, L. DelBuono, O. Leitner, and H. B. O'Connell, The dipion mass spectrum in e^+e^- annihilation and τ decay: A dynamical (ρ, ω, ϕ) mixing approach, Eur. Phys. J. C **55**, 199 (2008).
[19] M. Ablikim *et al.* (BESIII Collaboration), Determination of the number of $\psi(3686)$ events at BESIII, Chin. Phys. C **42**, 023001 (2018).
[20] S. Agostinelli *et al.* (GEANT4 Collaboration), Geant4a simulation toolkit, Nucl. Instrum. Methods Phys. Res., Sect. A **506**, 250 (2003).
[21] J. Allison *et al.*, Geant4 developments and applications, IEEE Trans. Nucl. Sci. **53**, 270 (2006).
[22] Z. Y. Deng *et al.*, Object-Oriented BES detector simulation system, Chin. Phys. C **30**, 371 (2006).
[23] S. Jadach, B. Ward, and Z. Was, The precision Monte Carlo event generator KK for two fermion final states in e^+e^- collisions, Comput. Phys. Commun. **130**, 260 (2000); Coherent exclusive exponentiation for precision Monte Carlo calculations, Phys. Rev. D **63**, 113009 (2001).
[24] D. Lange, The EvtGen particle decay simulation package, Nucl. Instrum. Methods Phys. Res., Sect. A **462**, 152 (2001); R. G. Ping, Event generators at BESIII, Chin. Phys. C **32**, 599 (2008).
[25] J. C. Chen, G. S. Huang, X. R. Qi, D. H. Zhang, and Y. S. Zhu, Event generator for J/ψ and $\psi(2S)$ decay, Phys. Rev. D **62**, 034003 (2000).
[26] M. Ablikim *et al.* (BESIII Collaboration), Branching fraction measurements of χ_{c0} and χ_{c2} to $\pi^0\pi^0$ and $\eta\eta$, Phys. Rev. D **81**, 052005 (2010).
[27] M. Ablikim *et al.* (BESIII Collaboration), Measurement of higher-order multipole amplitudes in $\psi(3686) \to \gamma\chi_{1,2}$ with $\chi_{1,2} \to \gamma J/\psi$ and search for the transition $\eta_c(2S) \to \gamma J/\psi$, Phys. Rev. D **95**, 072004 (2017).
[28] M. Ablikim *et al.* (BESIII Collaboration), Search for hadronic transition $\chi_{cJ} \to \eta_c\pi^+\pi^-$ and observation of $\chi_{cJ} \to K\bar{K}\pi\pi\pi$, Phys. Rev. D **87**, 012002 (2013).